Journal Pre-proof

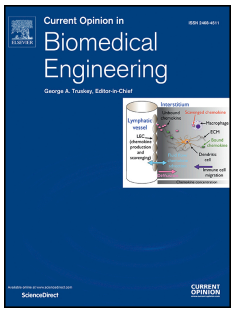

Multiscale Models of Kidney Function and Diseases

Anita T. Layton

PII: S2468-4511(19)30041-8

DOI: https://doi.org/10.1016/j.cobme.2019.09.006

Reference: COBME 174

To appear in: *Current Opinion in Biomedical Engineering*

Received Date: 3 May 2019

Revised Date: 22 August 2019

Accepted Date: 10 September 2019

Please cite this article as: A.T. Layton, Multiscale Models of Kidney Function and Diseases, *Current Opinion in Biomedical Engineering*, https://doi.org/10.1016/j.cobme.2019.09.006.

Multiscale Models of Kidney Function and Diseases

Running title: Multiscale Kidney Models

Anita T. Layton

Departments of Applied Mathematics and Biology, and School of Pharmacy, University of Waterloo, Waterloo, Ontario, Canada

Correspondence to Anita Layton

Department of Applied Mathematics, University of Waterloo

Waterloo, Ontario, Canada N2L 3G1

anita.layton@uwaterloo.ca

Abstract

The kidney is a complex system whose function is the result of synergistic operations among a number of biological processes. The spatial and functional scales of those processes span a wide range. To interrogate kidney function, one may apply multiscale models. Such models typically couple subcellular processes mediated by membrane channels and transporters, cellular processes, and supracellular processes such as nephron transport and renal autoregulation. We describe the approaches by which biological processes across scales can be coupled, and we highlight the successes of these multiscale models in revealing insights into kidney function under physiological, pathophysiological, or therapeutic conditions.

Introduction

Physiological systems are inherently complex, comprising of multiple functional units that operate across diverse temporal and spatial domains to sustain the life and activities of an organism. The kidney is one such complex system. Kidneys are commonly recognized as filters, removing metabolic wastes and toxins from blood and excreting them through urine. But the kidneys also serve other essential functions. Through a number of regulatory mechanisms, the kidneys help maintain the body's water balance, electrolyte balance, and acid-base balance. Additionally, the kidneys produce or activate hormones that are involved in erythrogenesis, calcium metabolism, and blood pressure regulation.

This review focuses on the mammalian kidney. The functional unit of the kidney is the nephron (see illustration under "organ-scale model" in Fig. 1). Each human kidney is populated by about a million nephrons. Each nephron consists of an initial filtering component called the renal corpuscle and a renal tubule specialized for reabsorption and secretion. The renal corpuscle is the site of formation of the glomerular filtrate, and is composed of a glomerulus, which is a tufts of capillaries arising from the afferent arterioles, and Bowman's capsule. A fraction of the water and solutes in the blood supplied by the afferent arteriole is driven by pressure gradients into the space formed by Bowman's capsule. The remainder of the blood flows into the efferent arteriole.

The renal tubule is the portion of the nephron in which the tubular fluid filtered through the glomerulus circulates before being excreted as urine. The role of the renal tubule is to adjust the composition of the filtrate. This adjustment takes place as the filtrate flows along the tubules, where reabsorption (i.e., removed from the filtrate, back into the interstitium, and

then into the circulation) of water and some solutes and secretion (i.e., released into the tubular fluid) of other solutes occurs. The tubular segments are lined by an epithelial cell barrier, which mediates water and solute exchanges between the tubular lumen and the surrounding interstitium.

Overall structure of multiscale kidney models

To illustrate the need for multiscale models in understanding kidney function, consider the multiple levels of spatial scale that are known to operate in the pathophysiology of *diabetes*. At the onset of diabetes, glomerular filtration is elevated (a.k.a. hyperfiltration). This symptom, observable at the macroscopic level, is driven by cellular hypertrophy and by changes in membrane transport at the subcellular level. To better understand the underlying mechanisms by which diabetes impairs kidney function, one may focus on a given level of resolution at which one believes most information can be gained. Alternatively, multiscale models may be built where perturbations to fine-grained parameters (e.g. protein modifications) can generate observable and measurable changes to coarse-grained outputs (e.g. glomerular filtration rate [GFR] or urine flow), and vice versa.

For kidney models, the hierarchy is typically grouped in terms of spatial dimensions, not temporal. These models are then linked together numerically across the scales. The structure of a multiscale kidney function model is illustrated in Fig. 1. Typically, at the macroscale are the organ-level models, which describe physiological processes that are essential for integrative kidney function, such as (i) renal autoregulation (1; 2; 3; 4; 5), which is the kidney's ability to maintain an approximately constant GFR despite changes in arteriolar pressure, (ii) renal

oxygenation and metabolism (6; 7; 8; 9; 10; 11; 12; 13), which largely depends, respectively, on blood flow and tubular active transport, and (iii) urine concentrating mechanism (14; 15; 16; 17; 18; 19; 20; 21; 22; 23), which refers to the kidney's ability to produce a urine that is much more concentrated than blood plasma during periods of water deprivation. Essentially, given a set of physiological or pathophysiological conditions, an organ-level model may predict GFR, renal oxygen consumption and tissue oxygen tension, and/or urine output and excretion.

It is fair to say that the engine behind the kidney function described above is the endothelial and epithelial cells. Endothelial cells of the afferent arteriole and descending vasa recta play a major role in autoregulation of renal and medullary blood flow, and thus oxygen delivery. Epithelial cells that form the nephron are responsible for transporting the majority of the filtered water and solutes, and for eventually producing a urine with a flow rate and composition that suits the animal's needs. This review focuses on multiscale models that involve epithelial transport. These models incorporate cellular-scale models that describe detailed transport processes and metabolism.

A notable feature of the nephron is its heterogeneity: the nephron consists of a number of functionally distinct segments, with different segments expressing a distinct set of transporters on the apical and basolateral membranes. These transporters mediate water and solute transport across the renal epithelia. Examples of such transporters include aquaporins (a family of small water permeable channels), Na^+,K^+-ATPase pumps, and various co-transporters (e.g., the Na^+-Cl^- cotransporter along the distal convoluted tubule) and antiporters (e.g., the Na^+/H^+ exchanger along the proximal tubule). Thus, at the subcellular or microscopic level, one

may formulate transport-scale models to predict transmembrane fluxes. The net fluxes computed over all transporters associated with a given cell yield its transepithelial transport.

Below we highlight published mathematical models at the transporter scale, cellular scale, and organ scale. Also, we discuss the bridging among models at different scales.

Transporter-scale models

Membrane proteins mediate transmembrane water and solute transport. Water transport is mediated by aquaporins and is predominantly osmotically driven. Hydraulic (ΔP) and oncotic ($\Delta\Pi$) pressure differences may both be significant across epithelial membranes. Thus, the water flux across aquaporins is determined as:

$$J_V^{\mathrm{AQP}} = L_p^{\mathrm{AQP}}(\Delta P - \Delta\Pi - \mathrm{RT}\sum_{\mathrm{ss}}\gamma_{\mathrm{ss}}\,\Delta C_{\mathrm{ss}}) \quad (1)$$

where L_p^{AQP} is the permeability of aquaporins to water, the subscript "ss" denotes small solutes, γ denotes solute activity coefficient, *C* denotes solute concentration, *R* is the universal gas constant, and *T* denotes temperature in K.

Transmembrane solute transport may be mediated by (i) channel proteins, which transport solutes down their concentration or electric potential gradients, (ii) pumps, which are ATPases that use the energy of ATP hydrolysis to move ions or small molecules across a membrane *against* a chemical concentration gradient or electric potential, or (iii) transporters, which move a wide variety of ions and molecules across cell membranes by undergoing a conformational change.

One class of renal transporter proteins are the antiporters, which transport two or more types of ions or molecules in opposite directions. We will illustrate how to build a transporter

model using as an example the luminal Na^+/H^+ exchanger of the proximal tubule (an acid-extruder). The kinetic diagram of Na^+/H^+ exchanger, shown in Fig. 2, accounts for the competitive binding of NH_4^+ and H^+; X is the empty transporter. The superscript "i" denotes the internal face of the membrane, and "e" the external face. The key assumption of the model is that ion binding is very rapid relative to membrane translocation. It is also assumed that the internal and external binding affinities are identical, but the equations can be easily modified to account for non-symmetric binding. With this formulation, knowing the binding equilibrium constants, the translocation rates, and the total amount of carrier, the fluxes can be calculated as a function of internal and external concentrations (24). Specifically, the outward flux of Na^+ is given by

$$J_{\mathrm{Na}}^{\mathrm{NHE}} = \frac{x_T T_{\mathrm{Na}}}{\Sigma}\left[T_{\mathrm{H}}\left(\alpha^i\beta^e + \alpha^e\beta^i\right) + T_{\mathrm{NH4}}\left(\alpha^i\gamma^e + \alpha^e\gamma^i\right)\right] \quad (2)$$

where x_T denotes the total amount of carrier (a conserved quantity), T_k represents the translocation rate of solute *k*,

$$\alpha^j = \frac{[\mathrm{Na}X]^j}{[X]^j}, \qquad \beta^j = \frac{[\mathrm{H}X]^j}{[X]^j}, \qquad \gamma^j = \frac{[\mathrm{NH_4}X]^j}{[X]^j},$$

where the superscript *j* = '*i*' *or* '*e*', and

$$\Sigma = \left(1 + \alpha^i + \beta^i + \gamma^i\right)\left(T_{\mathrm{Na}}\alpha^e + T_{\mathrm{H}}\beta^e + T_{\mathrm{NH4}}\gamma^e\right) + \left(1 + \alpha^e + \beta^e + \gamma^e\right)\left(T_{\mathrm{Na}}\alpha^i + T_{\mathrm{H}}\beta^i + T_{\mathrm{NH4}}\gamma^i\right)$$

Similarly, the outward fluxes of H^+ and NH_4^+ are given by

$$J_{\mathrm{H}}^{\mathrm{NHE}} = \frac{x_T T_{\mathrm{H}}}{\Sigma}\left[T_{\mathrm{Na}}\left(\alpha^e\beta^i + \alpha^i\beta^e\right) + T_{\mathrm{NH4}}\left(\beta^i\gamma^e + \beta^e\gamma^i\right)\right] \quad (3)$$

$$J_{\mathrm{NH4}}^{\mathrm{NHE}} = \frac{x_T T_{\mathrm{NH4}}}{\Sigma}\left[T_{\mathrm{Na}}\left(\alpha^e\gamma^i + \alpha^i\gamma^e\right) + T_{\mathrm{H}}\left(\beta^e\gamma^i + \beta^i\gamma^e\right)\right] \quad (4)$$

Thus, knowing the binding equilibrium constants, the translocation rates, and the total

amount of carrier, the fluxes are calculated as a function of internal and external concentrations.

Coupling between transporter-scale and cellular-scale models. Subcellular-scale transporter models predict water and solute fluxes. Solute fluxes are summed over each membrane (apical, basolateral) of every cell to yield the net transmembrane flux. See the brown arrow between the transporter-scale and cellular-scale models in Fig. 3 and the accompanying text. Consider as yet another example the apical Na^+ flux of a proximal convoluted tubule cell. The apical membrane transporters that media Na^+ transport include: Na^+/H^+ exchanger, Na^+-glucose cotransporter, and Na^+-$H_2PO_4^-$ cotransporter. Given the fluid composition of the luminal and cellular compartments, and membrane potential, each of these transporter models predicts its own transmembrane Na^+ flux. By summing all these fluxes, one obtains the net Na^+ across the apical membrane of the proximal convoluted cell. Other transmembrane solute fluxes across the apical and basolateral membranes can be determined using the same approach.

Cellular-scale models

In order to predict transport rates across the tubular epithelium, we must determine solute concentrations, volume, and electrical potential along tubules in the epithelial cells. These variables are obtained by solving conservation equations for mass, volume, and charge, respectively.

Epithelial cells exchange with the tubular lumen on the apical side, and with the peritubular fluid (or interstitium) and the lateral space between cells on the basolateral side.

We denote by *N* its surrounding compartments. The volume of the cell cytosol (V^{cell}) can expand and contract based on the amount of fluid accumulated during the time interval:

$$\frac{\partial V^{\text{cell}}}{\partial t} = \sum_N A^{\text{cell-}N} J_V^{\text{cell-}N} \quad (5)$$

where $A^{\text{cell-}N}$ is the surface area at the interface between the cell compartment and compartment, and $J_V^{\text{cell-}N}$ is the flux of volume from *N* into the cell, determined by the aquaporin models (Eq. 1).

Similarly, the rate of a given solute *S* that accumulates within the cytosol is given by the net flow of *S* into the cell, plus the net rate of *S* formation by chemical reaction within the cell:

$$\frac{\partial (V^{\text{cell}} C_S^{\text{cell}})}{\partial t} = \sum_N A^{\text{cell-}N} J_S^{\text{cell-}N} + V^{\text{cell}} \Phi_S^{\text{cell}} \quad (6)$$

where $J_S^{\text{cell-}N}$ is the molar flux of solute *S* from compartment *N* to cell, given by the sum of the *S* fluxes mediated by all the transporters on the cell-*N* membrane that mediate the transport of *S*. $J_S^{\text{cell-}N}$ can be computed using a transporter-scale model. Φ_S^{cell} is the volumetric rate of net generation of *S* within the cytosol.

For conservation of electric charge, macro-electroneutrality is imposed:

$$\sum_S z_S C_S^{\text{cell}} = 0 \quad (7)$$

where z_S denotes the valence of solute *S*.

A stand-alone epithelial cell model predicts changes in intracellular fluid composition and membrane potential, assuming that the environment surrounding cell is known; i.e., compositions of the fluids surrounding the bathing the apical membrane (luminal fluid) and the basolateral membrane (interstitial fluid) are assumed known. While this assumption may limit the capability of these models, they have nonetheless been used to predict how the circadian

rhythm found in the expression level of the Na^+/H^+ exchanger may affect proximal tubule cell transport (25), how the cell volume regulation mechanism of the proximal tubule cell helps it regulate water and solute transport under varying external conditions (26), and how thick ascending limb cell Na^+ transport may vary depending on luminal fluid composition (27). This modeling approach is by no means limited to epithelial cells and can be applied to model endothelial or smooth muscle cells as well (28).

Coupling between cellular-scale and organ-scale models. The cellular-scale models described above predict transepithelial and paracellular solute and water fluxes. To simulate kidney function, processes of individual cells must be combined to yield the collective actions. To that end, we link a number of cells in series to form a nephron model; see the brown arrow between the cellular-scale and organ/nephron-scale models in Fig. 3. Then we simulate a population of functionally distinct nephrons to predict kidney function.

Organ-level models

Organ-level models describe physiological processes that are essential for kidney function, such as renal autoregulation, oxygenation and metabolism, and urine concentrating mechanism. As previously noted, the functional unit of the kidney is the nephron. Nephrons can be classified based on their distinct anatomic and functional characteristics. To predict kidney function, one may combine a (relatively small) number of representative, functionally distinct nephron models. Below we describe how to formulate a nephron model, and how to extend a nephron model to a kidney model.

A nephron model allows one to predict solute concentrations, volume, and electrical potential along tubules, not only in the epithelial cells but also in the tubular lumen. Model equations that describe changes in cellular composition have been described above. Below we describe equations that predict luminal fluid composition. Along the lumen, let $F_V(x, t)$ and $C_S^{\text{lumen}}(x,t)$ respectively denote the fluid flow and the concentration of solute *S* in the tubular lumen at position x and time t. Assuming that the tubule is rigid, water conservation is given by

$$\frac{\partial F_V}{\partial x} = 2\pi r \left(A^{\text{lumen-cell}} J_V^{\text{lumen-cell}} + A^{\text{lumen-LIS}} J_V^{\text{lumen-LIS}} \right) \quad (8)$$

where the superscript LIS denotes lateral inner space, and *r* is the tubular radius. Similarly, the conservation of solute is given by:

$$\pi \frac{\partial (r^2 C_S^{\text{lumen}})}{\partial t} = \frac{\partial (F_V C_S^{\text{lumen}})}{\partial x} + 2\pi r \left(A^{\text{lumen-cell}} J_S^{\text{lumen-cell}} + A^{\text{lumen-LIS}} J_S^{\text{lumen-LIS}} \right) + \pi r^2 \Phi_S^{\text{lumen}} \quad (9)$$

where Φ_S^{lumen} is the volumetric rate of net generation of solute *S* in the tubular lumen.

For conservation of electric charge, open-circuit conditions, i.e., no net current into the lumen, are imposed:

$$\sum_S z_S \left(A^{\text{lumen-cell}} J_S^{\text{lumen-cell}} + A^{\text{lumen-LIS}} J_S^{\text{lumen-LIS}} \right) = 0 \quad (10)$$

By connecting a number of cell models in series, one can build a model of a nephron segment (e.g., (29; 30; 31)) or an entire nephron (e.g., (32; 33)). These models can predict how the composition of the luminal and intracellular fluid changes along the nephron segment or nephron. However, the composition of interstitial fluid is assumed known. Also, the kidney contains populations of functionally distinct nephrons (i.e., with distinct transport properties);

thus, a nephron model that represents only one type of nephrons cannot accurately predict overall kidney function. Despite these limitations, nephron models can provide insights into how nephron function may change under pathophysiological or therapeutic conditions (32; 33). All the aforementioned models are based on the rat, whose kidney is likely the most well studied. Compared to the rat, data in the human kidney is much sparser. Nevertheless, a computational model of epithelial transport along a human nephron (34) has recently been developed.

To assess whole-kidney function, one must represent nephrons from distinct populations. Such nephron populations include superficial nephrons having a loop of Henle that turns within a narrow boundary between the outer and inner medulla, and representative juxtamedullary nephrons having loops of Henle that reach into differing depths of the inner medulla (35). Single-nephron GFR is known to be different between superficial and juxtamedullary nephrons. Also, two juxtamedullary nephrons with loops of Henle of different lengths, say a shorter one that turns early in the inner medulla and a longer one that reach into the papillary tip, will have significantly different transport along those loops. Consequently, water and solute deliveries to segments downstream of the loops of Henle will also be significantly different between these two nephrons.

The nephron models and nephron population models above assume that the interstitial fluid composition is known *a priori*. As a result, those models do not predict interactions among nephrons; that is, transport changes in one nephron will not affect another nephron, because the interstitium that separates the two nephrons is assigned a fixed fluid composition. To simulate nephron-nephron interactions, interstitium fluid composition must be determined as a

function of nephron transport. One may also represent renal vasculature, which surround the nephrons, as was done in a recent whole-kidney model (36).

Perspectives

Multiscale multinephron models have been developed and applied to reveal insights into kidney function under pathophysiological and pharmaceutical conditions. One study (37) considers how kidney function changes when a significant fraction of the nephrons have been removed due to disease or surgery. Loss of renal mass stimulates anatomical and functional adaptations in the surviving nephrons (38). Model simulations indicate that such adaptations, which include increase in single-nephron GFR and tubular hypertrophy, go a long way to normalize urinary excretion, but alone are insufficient to fully maintain salt balance. Simulation results further indicate that, for the uninephrectomized and 5/6-nephrectomized models to achieve water and salt balance, i.e., to predict urine flow and urinary Na^+ and K^+ excretions that are similar to sham levels, the protein density of Na^+-K^+-ATPase, Na^+-K^+-$2Cl^-$ cotransporter, Na^+-Cl^- cotransporter, and epithelial Na^+ channel may need to be increased (37; 39).

In another study (40; 35), a multiscale multinephron model was applied to investigate the extent to which inhibitors of transepithelial Na^+ transport along the nephron alter urinary solute excretion and Na^+ transport efficiency and how those effects may vary along different nephron segments. Particularly noteworthy is the model prediction that whole-kidney Na^+ transport efficiency decreased by ~20% with 80% inhibition of Na^+/H^+-exchanger.

A recent study (41) seeks to predict the effects of SGLT2 inhibitors in diabetic patients with chronic kidney disease. Sodium-glucose cotransporter 2 (SGLT2) inhibitors enhance urinary

glucose, Na^+ and fluid excretion, and lower hyperglycemia in diabetes by targeting Na^+ and glucose reabsorption along the proximal convoluted tubule. Multiscale model simulations were conducted to explore how SGLT2 inhibition affects renal solute transport and metabolism when nephron populations are normal or reduced. Nephron loss in a diabetic kidney was predicted to lower the glucosuric and blood glucose-reducing effect of chronic SGLT2 inhibition, but due to the high luminal glucose delivery in the remaining hyperfiltering nephrons, nephron loss enhanced proximal tubular paracellular Na^+ secretion, thereby augmenting the natriuretic, diuretic, and kaliuretic effects.

Looking forward, a multiscale kidney model can be used as an integral component in comprehensive whole-animal models. As noted previously, the kidneys play a key role in blood regulation. Some long-term blood pressure regulation models include simple representation of the circulatory system, the renin-angiotensin system, the renal sympathetic nervous system, and the kidney (e.g., (42; 43)); see Fig. 4. By replacing the simple kidney model with a detailed multiscale model, one may more accurate simulate and predict the impacts on blood pressure of therapeutic maneuvers that target the kidneys. This is a worthwhile pursuit, despite the likely high computational costs.

Acknowledgement

This research was supported by the Canada 150 Research Chair program and by the National Institutes of Health via National Institute of Diabetes and Digestive and Kidney Diseases, grant R01DK106102.

Disclosure

The author declares no conflict of interest.

Bibliography

1. *Theoretical assessment of renal autoregulatory mechanisms.* **I Sgouralis, AT Layton.** 11, 2014, Am J Physiol Renal Physiol, Vol. 306, pp. F1357-F1371.
2. *Multistable dynamics mediated by tubuloglomerular feedback in a model of coupled nephrons.* **AT Layton, LC Moore, HE Layton.** 2009, Bull Math Biol, Vol. 71, pp. 515-555.
3. *Autoregulation and conduction of vasomotor responses in a mathematical model of the rat afferent arteriole.* **I Sgouralis, AT Layton.** 2, 2012, Am J Physiol Renal Physiol, Vol. 303, pp. F229-F239.
4. *Multistability in tubuloglomerular feedback and spectral complexity in spontaneously hypertensive rats.* **AT Layton, LC Moore, HE Layton.** 2006, Am J Physiol Renal Physiol, Vol. 291, pp. F79-F97.
5. *Feedback-mediated dynamics in a model of a compliant thick ascending limb.* **Layton, AT.** 2, 2010, Math Biosci, Vol. 228, pp. 185-194.
6. *Impact of renal medullary three-dimensional architecture on oxygen transport.* **BC Fry, A Edwards, I Sgouralis, AT Layton.** 3, 2014, Am J Physiol Renal Physiol, Vol. 307, pp. F263-F272 .
7. *Renal hemodynamics, function, and oxygenation during cardiac surgery performed on cardiopulmonary bypass: a modeling study.* **I Sgouralis, RG Evans, BS Gardiner, JA Smith, BC Fry, AT Layton.** 2015, Physiological reports, Vol. 3, p. e12260.
8. *Impacts of nitric oxide and superoxide on renal medullary oxygen transport and urine concentration.* **BC Fry, A Edwards, AT Layton.** 2015, Am J Physiol Renal Physiol, Vol. 308, pp. F967-F980.
9. *Impact of nitric-oxide-mediated vasodilation and oxidative stress on renal medullary oxygenation: a modeling study.* **BC Fry, A Edwards, AT Layton.** 2015, Am J Physiol Renal Physiol, Vol. 310, pp. F237-F247.
10. *A mathematical model of O2 transport in the rat outer medulla. I. Model formulation and baseline results.* **J Chen, AT Layton, A Edwards.** 2009, Am J Physiol Renal Physiol, Vol. 297, pp. F517-F536.
11. *A mathematical model of O2 transport in the rat outer medulla. II. Impact of outer medullary architecture.* **J Chen, A Edwards, AT Layton.** 2009, Am J Physiol Renal Physiol, Vol. 297, pp. F537-F548.
12. *Effects of pH and medullary blood flow on oxygen transport and sodium reabsorption in the rat outer medulla.* **J Chen, A Edwards, AT Layton.** s.l. : Am J Physiol Renal Physiol, 2010, Vol. 296, pp. F1369-F1383.
13. **Sex-specific computational models of the spontaneously hypertensive rat kidneys: factors affecting nitric oxide bioavailability.* **Y Chen, JC Sullivan, A Edwards, AT Layton.** 2017, Am J Physiol Renal Physiol, Vol. 313, pp. F174-F183.

*This is the first sex-specific computational model of the rat kidney. It considers the implications of higher nitric oxide bioavailability in females in the context of hypertension and oxidative stress..
14. *A region-based mathematical model of the urine concentrating mechanism in the rat outer medulla. I. Formulation and base-case results.* **AT Layton, HE Layton.** 2005, Am J Physiol Renal Physiol, Vol. 289, pp. F1346-F1366.
15. *Two modes for concentrating urine in rat inner medulla.* **AT Layton, TL Pannabecker, WH Dantzler, HE Layton.** 4, 2004, Am J Physiol Renal Physiol, Vol. 287, pp. F816-F839.
16. *A mathematical model of the urine concentrating mechanism in the rat renal medulla. I. Formulation and base-case results.* **Layton, AT.** 2, s.l. : Am J Physiol Renal Physiol, 2010, Vol. 300, pp. F356-F371.
17. *A region-based mathematical model of the urine concentrating mechanism in the rat outer medulla. II. Parameter sensitivity and tubular inhomogeneity.* **AT Layton, HE Layton.** 2005, Am J Physiol Renal Physiol, Vol. 289, pp. F1367-F1381.
18. *Functional implications of the three-dimensional architecture of the rat renal inner medulla.* **AT Layton, TL Pannabecker, WH Dantzler, HE Layton.** 2010, Am J Phyisol Renal Physiol, Vol. 298, pp. F973-F987.
19. *Role of thin descending limb urea transport in renal urea handling and the urine concentrating mechanism.* **T Lei, L Zhou, AT Layton, H Zhou, X Zhao, L Bankir, B Yang.** 2011, Am J Physiol Renal Physiol, Vol. 301, pp. F1251-F1259.
20. *A region-based model framework for the rat urine concentrating mechanism.* **AT Layton, HE Layton.** 5, 2003, Bull Math Biol, Vol. 65, pp. 859-901.
21. *Urine concentrating mechanism: impact of vascular and tubular architecture and a proposed descending limb urea-Na+ cotransporter.* **AT Layton, WH Dantzler, TL Pannabecker.** 5, 2011, Am J Physiol Renal Physiol, Vol. 302, pp. F591-F605.
22. *Urine-concentrating mechanism in the inner medulla: function of the thin limbs of the loops of Henle.* **WH Dantzler, AT Layton, HE Layton, TL Pannabecker.** 10, 2014, Clin J Am Soc Nephrol, Vol. 9, pp. 1781-1789.
23. *A mathematical model of the urine concentrating mechanism in the rat renal medulla. II. Functional implications of three-dimensional architecture.* **Layton, AT.** 2, 2010, Am J Physiol Renal Physiol, Vol. 300, pp. F372-F384.
24. **AT Layton, A Edwards.** *Mathematical Modeling in Renal Physiology.* Berline : Springer, 2014.
25. *Predicted effect of circadian clock modulation of NHE3 of a proximal tubule cell on sodium transport.* **N Wei, ML Gumz, AT Layton.** 3, 2018, Am J Physiol Renal Physiol, Vol. 315, pp. F665-F676.
26. *Cell volume regulation in the proximal tubule of rat kidney.* **A Edwards, AT Layton.** 11, 2017, Bull Math Biol, Vol. 79, pp. 2512-2533.
27. *Fluid dilution and efficiency of Na+ transport in a mathematical model of a thick ascending limb cell.* **A Nieves-González, C Clausen, M Marcano, AT Layton, HE Layton, LC Moore.** 6, s.l. : Am J Physiol Renal Physiol, 2012, Vol. 304, pp. F634-F652.
28. *Calcium dynamics underlying the myogenic response of the renal afferent arteriole.* **A Edwards, AT Layton.** 2014, Am J Physiol Renal Physiol, Vol. 236, pp. 187-202.
29. ***Functional implications of sexual dimorphism of transporter patterns along the rat proximal tubule: modeling and analysis.* **Q Li, AA McDonough, HE Layton, AT Layton.** 3, 2018, Am J Physiol Renal Physiol, Vol. 315, pp. F692-F700.

**This study presents the first sex-specific computational model of solute and water transport along a major segment of the rat nephron. It reveals functional implications of sexual dimorphism of transporter patterns recently came into light..
30. *Effects of NKCC2 isoform regulation on NaCl transport in thick ascending limb and macula densa: a modeling study.* **A Edwards, H Castrop, K Laghmani, V Vallon, AT Layton.** 2, 2014, Am J Physiol Renal Physiol, Vol. 307, pp. F137-F146.
31. *Transport efficiency and workload distribution in a mathematical model of the thick ascending limb.* **A Nieves-González, C Clausen, AT Layton, HE Layton, LC Moore.** 6, 2012, Am J Physiol Renal Physiol, Vol. 304, pp. F653-F664.
32. *Modeling oxygen consumption in the proximal tubule: effects of NHE and SGLT2 inhibition.* **AT Layton, V Vallon, A Edwards.** 12, 2015, Am J Physiol Renal Physiol, Vol. 308, pp. F1343-F1357.
33. *Predicted consequences of diabetes and SGLT inhibition on transport and oxygen consumption along a rat nephron.* **AT Layton, V Vallon, A Edwards.** 11, 2016, Am J Physiol Renal Physiol, Vol. 310, pp. F1269-F1283.
34. ***A computational model of epithelial solute and water transport along a human nephron.* **AT Layton, HE Layton.** 2, 2019, PLoS Comput Biol, Vol. 15, p. e1006108.
**This is the first and so far only computational model of solute and water transport in the human kidney. .
35. *A computational model for simulating solute transport and oxygen consumption along the nephrons.* **AT Layton, V Vallon, A Edwards.** 6, 2016, Am J Physiol Renal Physiol, Vol. 311, pp. F1378-F1390.
36. *A mathematical model of the rat kidney: K+-induced natriuresis.* **Wesintein, AM.** 6, 2017, Am J Physiol Renal Physiol, Vol. 312, pp. F925-F950.
37. *Adaptive changes in GFR, tubular morphology, and transport in subtotal nephrectomized kidneys: modeling and analysis.* **AT Layton, A Edwards, V Vallon.** 2, 2017, Am J Physiol Renal Physiol, Vol. 313, pp. F199-F209.
38. *How do kidneys adapt to a deficit or loss in nephron number?* **H Fattah, A Layton, V Vallon.** 3, 2019, Physiology, Vol. 34, pp. 189-197.
39. *Renal potassium handling in rats with subtotal nephrectomy: Modeling and Analysis.* **AT Layton, A Edwards, V Vallon.** 4, 2017, Am J Physiol Renal Physiol, Vol. 314, pp. F643-F657.
40. *Solute transport and oxygen consumption along the nephrons: effects of Na+ transport inhibitors.* **AT Layton, K Laghmani, V Vallon, A Edwards.** 6, 2016, Am J Physiol Renal Physiol, Vol. 311, pp. F1217-F1229.
41. ***SGLT2 inhibition in a kidney with reduced nephron number: modeling and analysis of solute transport and metabolism.* **AT Layton, V Vallon.** 5, 2018, Am J Physiol Renal Physiol, Vol. 314, pp. F969-F984.
**This is an important study that explains why SGLT2 inhibitors may have cardiovascular benefits for patients with impaired kidney function..
42. *Circulation: overall regulation.* **AC Guyton, TG Coleman, HJ Granger.** 1, 1972, Ann Rev Physiol, Vol. 34, pp. 13-44.
43. **Sex-specific long-term blood pressure regulation: modeling and analysis.* **J Leete, AT Layton.** 2019, Computers Biol Med, Vol. 104, pp. 139-148.
*This study presents the first sex-specific computational model of long-term blood pressure control. Simulation results reveal mechanisms that explain why some antihypertensive drugs are more effective for men, and others for women..

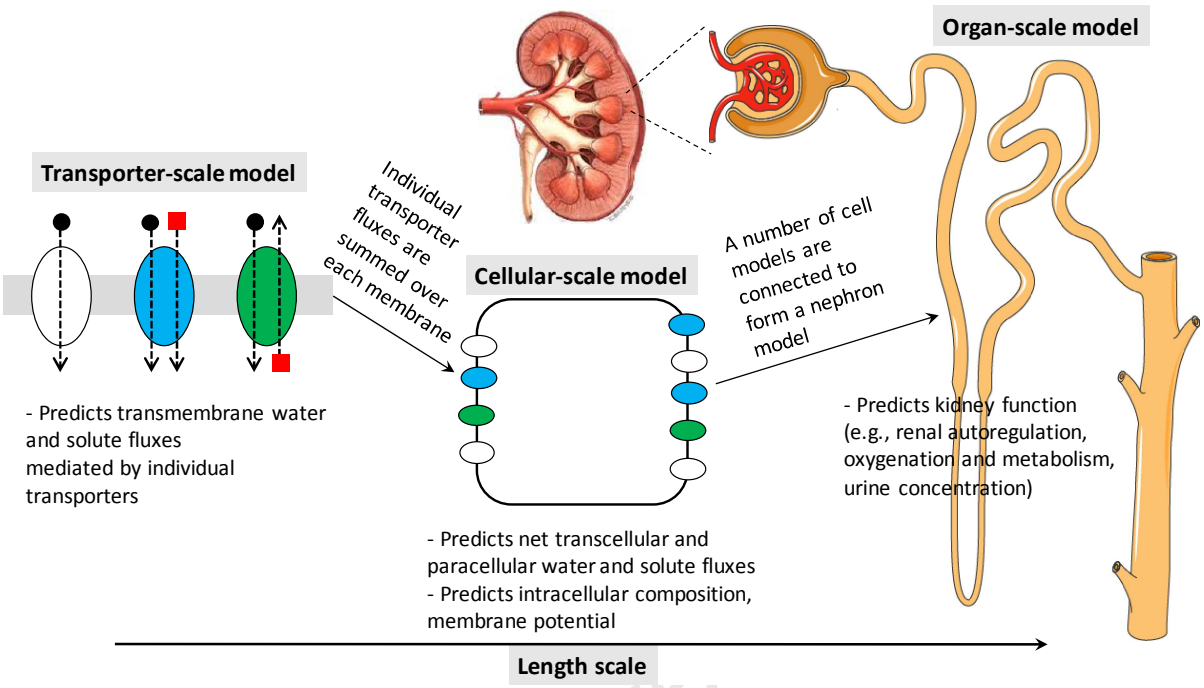

Figure 1. Structure of a multiscale kidney model, involving (subcellular/microscopic) transporter-scale, cellular-scale, and (supracellular/macroscopic) organ-scale models.

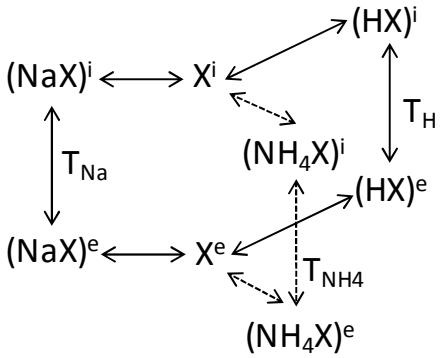

Figure 2. Model representation of the Na^+/H^+ exchanger. Na^+, H^+, and NH_4^+ bind to the empty carrier (X), and the resulting complexes are translocated across the membrane.

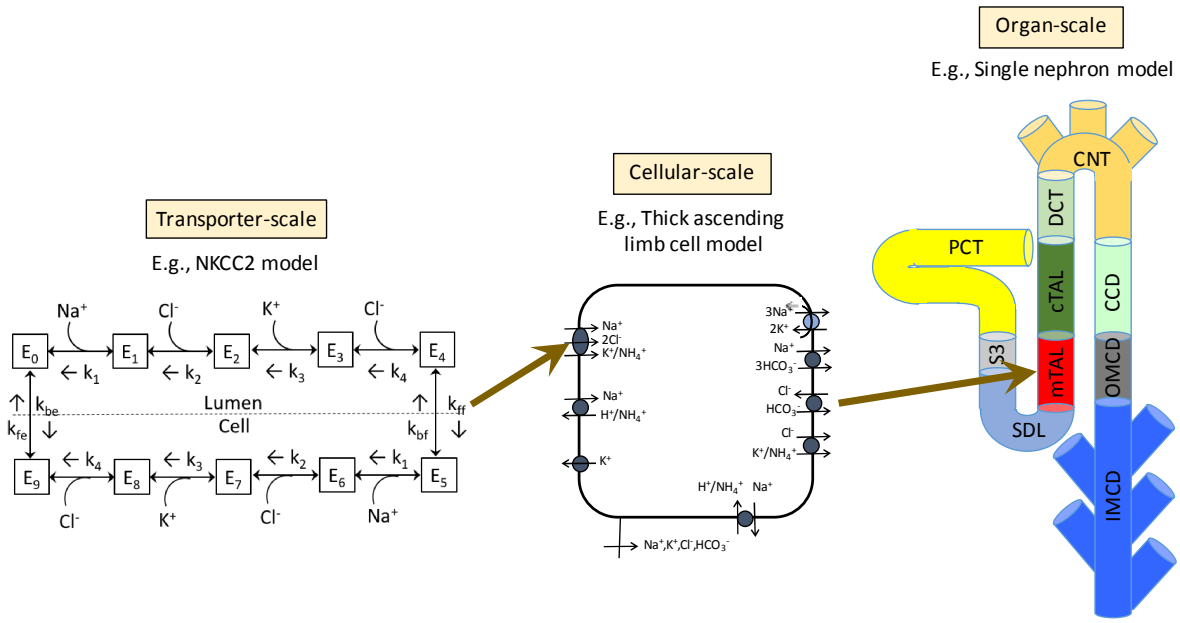

Figure 3. A multiscale kidney model, involving transporter-scale, cellular-scale, and organ-scale models. The Na^+-K^+-Cl^- cotransporter isoform 2 (NKCC2) is given an example of a *transporter-scale model*. NKCC2 is expressed on the apical membrane of the thick ascending limb cell. Fluxes predicted by the NKCC2 model and other transporter-scale models are used to determine transmembrane fluxes of the thick ascending limb cell, a *cellular-scale model*. A series of thick ascending limb models together form the thick ascending limb segment of the *organ-scale* single nephron model. Brown arrows indicate coupling between models of different scales.

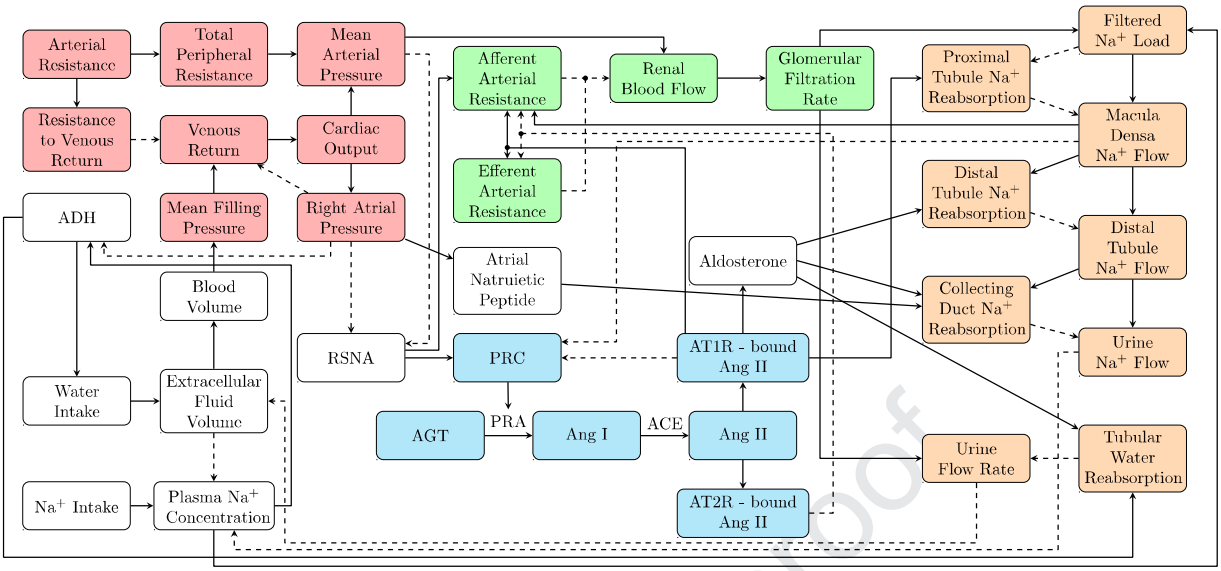

Figure 4. Schematic model of blood pressure regulation. Pink nodes denote variables that describe cardiovascular function; green nodes, renal hemodynamics; orange nodes, simple kidney model representing renal Na^+ handling and urine production; blue nodes, the renin-angiotensin system. ADH, anti-diuretic hormone; RSNA, renal sympathetic nerve activity; PRC, plasma renin concentration; PRA, plasma renin activity; AGT, angiotensinogen; Ang I, angiotensin I; Ang II, angiotensin II; AT1R-bound Ang II, angiotensin II type 1 receptor bound angiotensin II; AT2R-bound Ang II, angiotensin II type 2 receptor bound angiotensin II. Reprinted from (43).

Disclosure

The author declares no conflict of interest.